Geochemistry Geophysics Geosystems G3

Published by AGU and the Geochemical Society

Article
Volume 14, Number 6
5 June 2013
doi:10.1002/ggge.20082
ISSN: 1525-2027

High-resolution Remotely Operated Vehicle (ROV) mapping of a slow-spreading ridge: Mid-Atlantic Ridge 45°N

I. A. Yeo and R. C. Searle

Department of Earth Sciences, Durham University, Durham, UK (i.a.yeo@durham.ac.uk)

[1] Axial volcanic ridges (AVRs) are found on most slow-spreading mid-ocean ridges and are thought to be the main locus of volcanism there. In this study we present high-resolution mapping of a typical, well-defined AVR on the Mid-Atlantic Ridge at 45°N. The AVR is characterized by "hummocky terrain," composed typically of hummocks with pillowed or elongate pillowed flanks with pillowed or lobate lava flow summits, often with small haystacks sitting on their highest points. The AVR is surrounded by several areas of "flat seafloor," composed of lobate and sheet lava flows. The spatial and morphological differences between these areas indicate different eruption processes operating on and off the AVR. Volcanic fissures are found all around and on the AVR, although those with the greatest horizontal displacement are found on the ridge crest and flat seafloor. Clusters of fissures may represent volcanic vents. Extremely detailed comparisons of sediment coverage and examination of contact relations around the AVR suggest that many of the areas of flat seafloor are of a similar age or younger than the hummocky terrain of the AVR. Additionally, all the lavas surveyed have similar degrees of sediment cover, suggesting that the AVR was either built or resurfaced in the same 50 ka time frame as the flat seafloor.

Components: 6,014 words, 5 figures, 2 tables.

Keywords: Mid-Atlantic Ridge; axial volcanic ridge; Remotely-Operated Vehicle.

Index Terms: Submarine tectonics and volcanism.

Received 14 September 2012; **Revised** 25 January 2013; **Accepted** 31 January 2013; **Published** 5 June 2013.

Yeo, I. A., and R. C. Searle (2013), High-resolution ROV mapping of a slow-spreading ridge: Mid-Atlantic Ridge 45°N, *Geochem. Geophys. Geosyst.*, *14*, 1693–1702, doi:10.1002/ggge.20082.

1. Introduction

[2] Axial volcanic ridges (AVRs) have been recognized on most slow-spreading ridge segments [*Ballard and Van Andel*, 1977; *Bideau et al.*, 1998; *Briais et al.*, 2000; *Brown and Karson*, 1988; *Bryan et al.*, 1994; *Gente et al.*, 1989; *Gràcia et al.*, 1998; *Karson et al.*, 1987; *Parson et al.*, 1993; *Sempere et al.*, 1990; *Smith and Cann*, 1992]. AVRs are composite volcanic constructions, built entirely of small basaltic eruptions. They are typically several kilometers wide, tens of kilometers long, and up to a kilometer high [*Smith and Cann*, 1992, 1993].

[3] Significant advances in the understanding of mid-ocean ridge processes have been made using combinations of low-resolution shipboard bathymetry, medium-resolution deep-towed side-scan sonar, and high-resolution submersible or towed camera observations. The lower-resolution studies distinguished "smooth terrains" composed of low-relief lavas, from "hummocky morphology" composed

of thousands of small, discrete volcanoes [*Ballard and Van Andel*, 1977; *Smith and Cann*, 1990; *Smith et al*., 1995a, while higher-resolution studies described the morphology and spatial distribution of volcanic activity, landforms, and morphologies [e.g., *Ballard and Moore*, 1977]. However, few studies have focused specifically on AVRs (excepting *Parson et al*. [1993]) or comprehensively surveyed them, and their formation and life cycle remain poorly understood.

[4] AVR volcanism may produce lavas with a variety of morphologies, including pillow lavas, composed of an accumulation of bulbs, tubes, and lobes of solidified basalt; sheet flows; fairly flat, continuous flows; and lobate flows, characterized by a gentle, hummocky surface [*Ballard and Moore*, 1977; *Kennish and Lutz*, 1998]. Changing lava morphology has been linked to effusion rate, lava rheology, and underlying slope [*Gregg and Fink*, 1995]. Increasing effusion rate or decreasing viscosity is expected to favor the production of lobate and sheet flows [*Bonatti and Harrison*, 1988; *Griffiths and Fink*, 1992; *White et al*.,] and can also produce a more fluid pillow form [*Chadwick and Embley*, 1994]. Increasing slope from 0° to 30° has a similar effect; however, at > 40°, flows typically channelize and form lobes rather than smooth flows [*Gregg and Fink*, 2000]. Steep slopes can also disrupt flow fronts by pulling both molten and solid lavas apart, favoring the production of pillow or lobate lavas [*Gregg and Smith*, 2003]. Ponding of lava flows may also produce sheet flow textures.

[5] The spreading segment at 45°30′N is typical of the Mid-Atlantic Ridge. The median valley varies in width from 5 km at its center (45°28′N) to 8 km at its southern end (45°23′N) and 12 km at its northern end (45°37′N) and is characterized by a mature AVR (Figure 1). The hourglass-shaped axial valley is terminated at both ends by small dextral offsets (at 45°23′N and 45°42′N). The well-defined 22 km long AVR runs from 45°24′N to 45°35′N and reaches > 600 m above the surrounding seafloor. Sections, such as the eastern side of the axis between 45°35′N and 45°40′N may be characterized by detachment faulting [*Escartin et al*., 2008]. Previous studies [*Aumento et al*., 1971; *Keeton and Searle*, 1996; *Mello et al*., 1999; *Searle et al*., 2010] identified a number of different volcanic morphologies in the area and noted that the nature of the AVR changes from narrow, focused volcanism south of 45°33′N to less focused and more tectonized north of 45°33′N [*Searle et al*., 2010]. The AVR also displays good examples of flat seafloor and volcanic hummocks. Hummocks, described as 5–150 m high, 30–350 m diameter domes or cones, built predominantly of pillow lavas

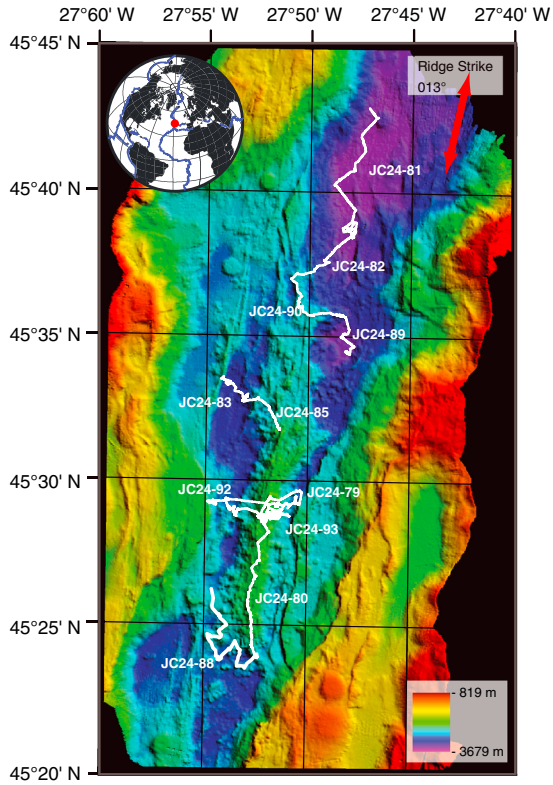

Figure 1. EM120 bathymetry for the ridge segment at 45°30′N on the Mid-Atlantic Ridge. Video dive tracks are shown in white, with their dive numbers.

[*Smith and Cann*, 1990; *Yeo et al*., 2012], are the most common style of volcanic edifice on slow-spreading mid-ocean ridges. These factors make the 45°30′N spreading segment ideal for studying various volcanic morphologies and for examining the differences between young and old-looking AVR terrains.

2. Data Acquisition and Methods

2.1. Data Acquisition

[6] Data were collected during RRS James Cook cruise 24 in May and June 2008. Side-scan sonar data were acquired using the Towed Ocean Bottom Instrument (TOBI) operated by NOC, Southampton, UK [*Flewellen et al*., 1993]. TOBI is fitted with 30 kHz side-scan sonar which measures 6 km wide swaths with a pixel size of ~3 m [*LeBas*, 2005]. Postprocessed data have an absolute navigational precision of 100 m. Twenty-two E-W, 2 km-spaced tracks provided 100% N- and S-looking sonar coverage (Appendix A in the auxiliary material). Attenuation of TOBI backscatter can be used as a proxy for sediment thickness and therefore age. Data were interpreted by *Searle et al*. [2010].

[7] Video data were captured by two cameras using the ROV Isis (operated by NOC, Southampton, UK; [*German et al.*, 2003]). Video was recorded at all times during 11 sampling dives (dives 79, 80, 81, 82, 83, 85, 88, 89, 90, 92, and 93). Three dives (centered on 45°29.0′N, 27°51.5′W) were in an area of Simrad SM2000 microbathymetry collected by the ROV. It has postprocessed horizontal and vertical resolution of ~1–2 m [*Searle et al.*, 2010].

[8] Video and sampling dives were carried out in both the robust southern AVR and the tectonized north, on the axial valley floor (Figure 1) and up the axial valley wall fault scarps (Figure 2). Sediment was recorded from visual observations. The dive positions were chosen based on the TOBI side-scan sonar and, where it was available, high-resolution SM2000 bathymetry.

2.2. Mapping

[9] Lava morphology was split into seven categories, including pillow lavas (Figures 3a and 3b), elongate pillow lavas (Figure 3c), lobate lavas (Figure 3d), and sheet flows (Figures 3e and 3f). Scarps (Figure 3g), talus (Figure 3h), and total sediment cover (Figure 3i) were also recorded. Frequently two lava types would occur close together, and where both were observed within a 10 m^2 area, we used the additional categories pillow and elongate pillow lavas, pillow and lobate lavas, and lobate and sheet flows.

[10] Sheeted lava flows were not divided further (i.e., into ropey, lineated, etc.) as they are more easily buried by sediment and exposures were typically not large enough to be representative of the whole flow. Scarps were defined as any broken vertical or near-vertical face. Fissures were defined as any crack cutting the seafloor and were subdivided into those which were purely eruptive, i.e., those that were narrow, sinuous, surrounded by pillow lavas, and formed a local high and those which were linear, purely tectonic cracks, or previously eruptive fissures with large horizontal opening. We also mapped haystacks, cone-shaped features < 5 m high, composed of pillows and elongate pillows, and collapse pits.

[11] The first-order along-track mapping was done using the Adelie-Otus ArcGIS extension developed by

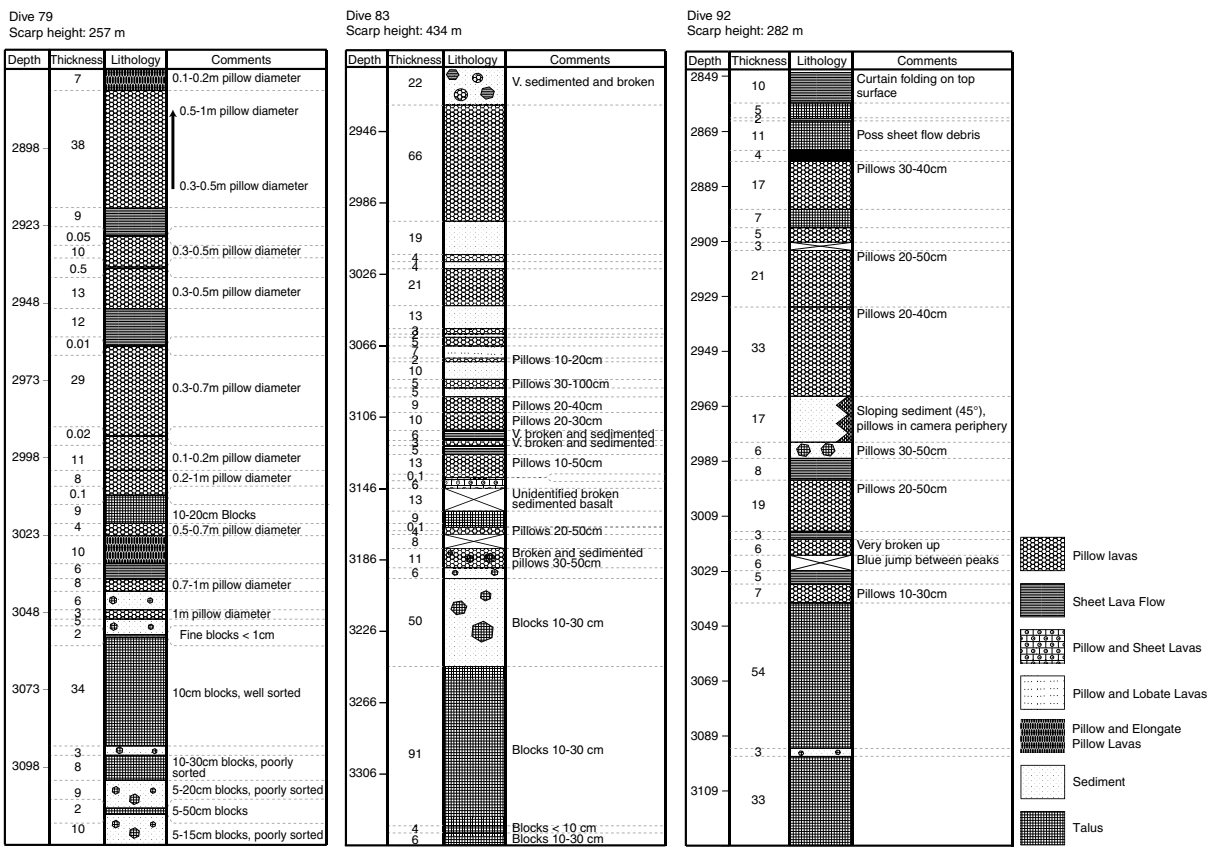

Figure 2. Scarp morphology logs of the three sections of axial valley wall scarp observed on dives 79, 83, and 92.

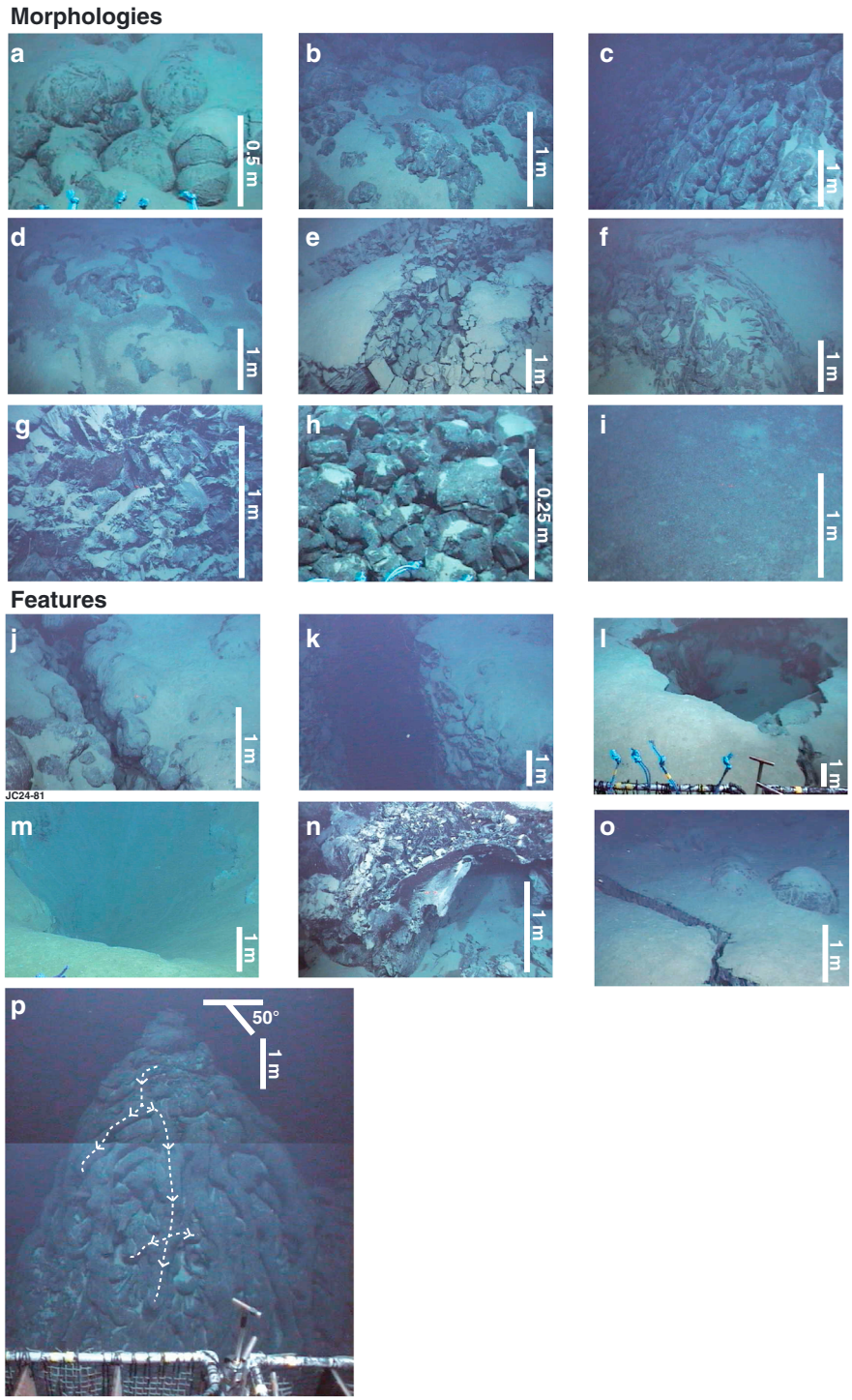

Figure 3. Typical lava morphologies and features observed on the sampling dives. (a) Pillow lavas (dive 82), (b) pillow lavas (dive 90), (c) elongate pillow lavas (dive 88), (d) lobate lava flows (dive 82), (e) broken sheet flow (dive 83), (f) textured sheet flow surface (dive 82), (g) broken lavas in a fault scarp wall (dive 81), (h) talus deposit at the base of a fault scarp (dive 80), (i) 100% sediment cover (dive 82), (j) eruptive fissure (dive 81), (k) non-eruptive crack on the seafloor (dive 81), (l) trapdoor (dive 89), (m) collapse pit (dive 81), (n) lava tube (dive 89), (o) sheet flow lavas (seen in fissure) with associated pillow lavas visible through the thin sediment layer covering their surface (dive 81), (p) haystack (dashed lines show the length of a single pillow) (dive 92).

L'Institut Français de Recherche pour l'Exploitation de la Mer (IFREMER), Brest, mounted on an ArcGIS 9.1 platform. Further maps were produced using ArcGIS and Adobe Illustrator CS3. Seafloor Morphology was recorded at 1 min intervals during dives, which, with a typical ROV speed of ~1 km/h, equates to one observation every ~17 m. This is the smallest scale at which meaningful lithological changes can be observed and is similar to the resolution of the TOBI survey. Strikes were recorded for structural features observed. These have variable accuracy as some were measured with the ROV while others are estimated relative to the vehicle heading. This second type has an estimated accuracy of $\pm 20°$. Dive maps and descriptions can be found in Appendices B and C in the auxiliary material.

2.3. Sediment Cover

[12] In order to compare the sedimentation along and between dives [*Goldberg and Sun*, 1997; *Macdonald*, 1982; *Smallwood and White*, 1998], we devised a sedimentation scale. Sediment cover (SC) categories were assigned with divisions at 1 (< 10% sediment cover—light dusting of sediment), 2 (10–50% sediment cover—sediment on surfaces but no joined sediment pockets between lavas), 3 (50–90% sediment cover—heavy sediment cover with interconnected sediment pockets), and 4 (> 90% sediment cover). These categories do not represent regular divisions of sediment thickness, but are the clearest divisions observable from the video footage, as cross sections of sediment thickness are not usually visible. As with the morphology mapping, observations of sediment cover were made every minute along the video dives, except on vertical or near-vertical slopes where sediment is unable to settle. There is no way to remove errors associated with currents or differing deposition rates, so broad comparisons of lavas tens of kilometers apart are difficult; however, comparisons between lavas close to each other should be fairly reliable.

[13] This method differs to that used by *Cann and Smith* [2005] to examine sediment cover at 25°N because direct observations of the sediment thickness in cross section were not available at the resolution at which observations were made; however, the percentage cover could be recorded every minute, giving a higher resolution of sampling. These observations could be used as a proxy for sediment thickness and relative age when comparing similar terrains within a few hundreds of meters. In order to compare different types of flow, sediment thickness was used only where it was observed in cross section (i.e., at fissures/scarps).

3. Observations

[14] A detailed description of each dive is included in Appendix C in the auxiliary material. The general observations are summarized below.

3.1. Large-Scale Volcanic Morphology

[15] Volcanic hummocks with diameters 30–350 m were observed all over the AVR and on parts of the surrounding lower-lying terrain. Slopes on the flanks of hummocks were typically 20° to 40°, and their summits ranged from almost flat to up to 25°. Many were characterized by summit haystacks (Figure 3p).

[16] Flat seafloor, composed mainly of sheet and lobate lava flows, was observed around the AVR, particularly in the north. In some places pillow lavas can be observed forming on the top surfaces of sheet and lobate flows (Figure 3o). Pillow lavas were also observed in small discrete areas within the sheet flows, which appear to correlate to small hummocks observed in the side-scan sonar.

[17] Nineteen flat-topped seamounts are imaged in the EM120 data as mapped by *Searle et al.* [2010]. Flat-topped seamounts are predominantly observed around the AVR rather than on it (seven of the seamounts lie outside the AVR but still lie within the axial valley floor, only two lie on the AVR) and are distributed fairly evenly from north to south. Three flat-topped seamounts were dived on, two near 45°25.85′N, 27°54.45′W (dive 88) and one at 45°42.58′N, 27°46.52′W (dive 81). All of these were characterized by sloping (15–40°) pillowed or elongate pillowed lava flows on their flanks and sheet flow or lobate flows on their flat (< 10°) tops.

3.2. Fissures

[18] In order to distinguish between the types of fissure observed, we classify them as either "narrow" or "open." Narrow fissures consist of narrow, sinuous fissures with less than a meter of separation and pillows and lobate flows spilling out of them (Figure 3j). The open fissures (Figure 3k) are straighter and much wider (up to 15 m) and deeper (> 30 m), with vertical walls composed of broken pillow lava or broken sheet flow faces. This classification is purely given as a way to distinguish two separate morphologies of fissure, and some open fissures may have previously erupted—many had a mix of talus and pillows in their bases and pillows

on their edges. In some cases these larger fissures have small vertical offsets between the walls of the fissure. Of the fissures observed, almost all are parallel or close to the strike of the ridge (Figure 4), with 70% of measured strikes lying within ±25° of the AVR strike; the distribution of orientations of the narrow and open fissures is very similar.

[19] Skylights (places where the unsupported solidified crust over a drained lava flow collapses) (Figure 3l) and heavily sedimented collapse pits (Figure 3m) (which were of the same size and may be the sedimented skylights) were also observed associated with the sheet and lobate lava morphologies.

3.3. Fault Scarps

[20] Faults were observed on the axial valley walls, consisting of stepped vertical or near-vertical sections, from 5 m to several hundred meters in height. These terraces were composed of broken lavas, separated by small 2–5 m flat benches that were usually fairly heavily sedimented. These wall scarps produced quite extensive talus deposits extending away from their bases for up to 300 m. Smaller scarps, usually < 100 m in height, are also observed on the AVR as both faults and gravitational collapse scars on hummocks [*Yeo et al.*, 2012].

3.4. Sediment Distribution

[21] While flatter-lying lava flows often appeared more sedimented (typically between SC 3 and 4) (Figure 5), where broken surfaces were exposed, this sediment cover was shown to be usually < 10 cm, which would be comparable to SC 2 (10–50% cover) for the AVR pillow lavas. The lavas that appeared to have the thinnest sediment cover were observed on dive 88 on the southern and southwestern sections of the AVR and surrounding seafloor, with sediment cover of 10–60% (SC as young as 1 and 2) being observed. Lavas with no sediment cover were not observed anywhere.

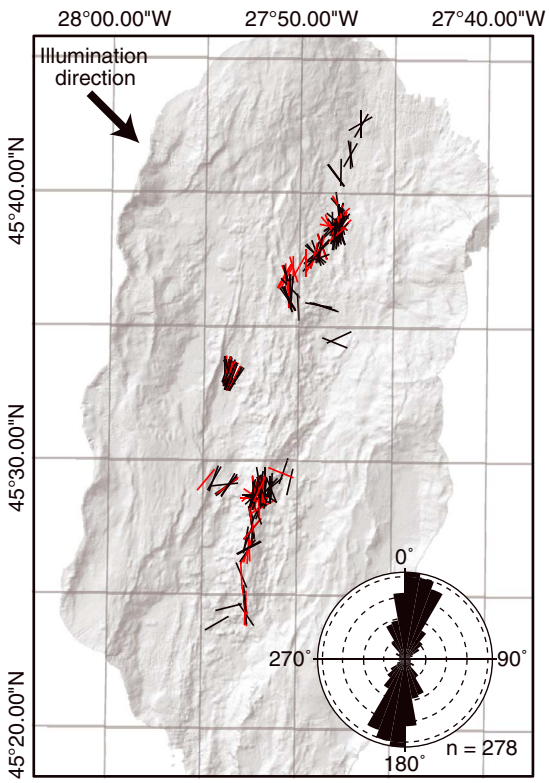

Figure 4. Fissure orientations for all dives. Narrow fissures are shown in black, open fissures (with horizontal widths > 1 m) are shown in red. Of the 277 fissures observed, 70% lie within 25° of the ridge strike.

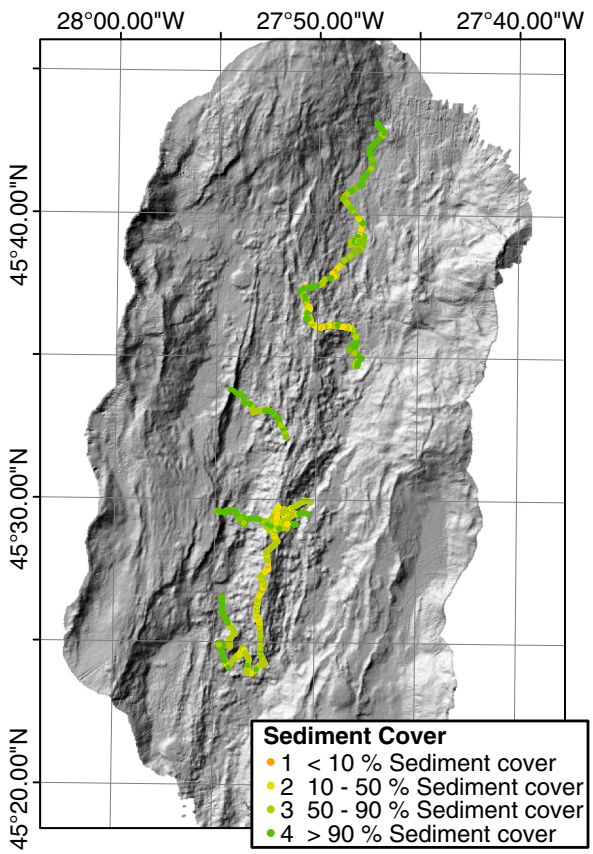

Figure 5. Sediment cover on all the dives. No lavas of sediment age 0 were observed. Sediment cover ages were recorded every minute and every point along the dive tracks represents one observation.

4. Discussion

4.1. Eruption Products

[22] The building blocks of the AVR at the Mid-Atlantic Ridge (MAR) 45°N are pillow, lobate, and very rarely sheet lava flows (Table 1), as found elsewhere on the MAR [*Ballard and Moore*, 1977; *Ballard and Van Andel*, 1977; *Briais et al.*, 2000; *Brown and Karson*, 1988; *Sinton and Detrick*, 1992; *Smith and Cann*, 1990, 1993].

[23] Pillow lavas form the main building blocks of hummocks (Table 2) and were additionally observed on the flanks of flat-topped seamounts and in areas of flat seafloor, suggesting that multiple lava morphologies can be produced by the same flow. Elongate pillow lavas are observed only on slopes over 15° and predominantly on those $> 20°$, consistent with observations elsewhere [*Kennish and Lutz*, 1998; *Wells et al.*, 1979].

[24] Sheet lava flows were observed only around the edges of the AVR [*Searle et al.*, 2010] or on the summits of flat-topped seamounts, where the seafloor is flat or very gently sloping ($< 10°$), suggesting that they are only produced on areas of low-gradient seafloor or that they produce such seafloor. Some areas of the flat seafloor appeared slightly hummocky, suggesting that they did have some (normally less than 10 m) relief. This may be due to the burial of hummocky terrain beneath these flows or be due to inflation (as evidenced by the observation of numerous tumuli) or deflation of the flow surface during the eruption.

[25] A clear relationship between textures observed in the TOBI side-scan sonar and the morphology observed on the ground can be seen in Table 1 and in the maps in Appendix B in the auxiliary material. The observation of a clear change in lava morphology with change in side-scan texture is in contrast to some of the observations from a similar study at 25°N [*Cann and Smith*, 2005]. Like we did, they find hummocky terrain to be composed of pillow lavas, but also observe only pillows on smooth side-scan terrains. This differs from our observations of single or small groups of pillows, which were commonly observed on the top surfaces of sheet flows at 45°N, but at a lower density than in the hummocky terrain. The flat, pillowed terrains described by Cann and Smith (2005) may overly sheet flows, possibly produced by burial of a sheet flow during the later stages of the same eruption or by separate eruptions that postdate the flow. Alternatively, the slightly thicker sedimentation at

Table 1. Measured Dive Length of Each Observed Lava Morphology as a Percentage of the Total Cumulative Dive Length for all the Dives Together, and for the Individual Dives[a]

	Elongate Pillow Lavas	Pillow and Elongate Pillow Lavas	Pillow Lavas	Pillow and Lobate Flows	Lobate Flows	Lobate and Sheet Flows	Sheet Flows
All dives	4	27	20	26	13	4	6
Dive 79	1	37	51	9	2	0	0
Dive 80	4	48	23	15	10	0	0
Dive 81	0	6	10	34	13	14	23
Dive 82	2	24	23	21	19	6	5
Dive 83	0	3	32	42	6	8	9
Dive 85	6	24	33	20	17	0	0
Dive 88	2	38	20	23	14	2	1
Dive 89	5	14	6	33	30	10	2
Dive 90	13	64	10	10	3	0	0
Dive 92	3	37	15	32	9	2	2
Dive 93	7	58	15	10	9	0	1

[a]Areas of scarp, talus, or sediment cover, and sections of the dives where the seafloor was not observed, were omitted from the measurements.

Table 2. Lava Morphology as a Percentage of Total Observed Morphology on Hummocky vs. Flat Seafloor[a]

	Elongate Pillow Lavas	Pillow and Elongate Pillow Lavas	Pillow Lavas	Pillow and Lobate Flows	Lobate Flows	Lobate and Sheet Flows	Sheet Flows
Hummocky seafloor	5	36	24	23	12	0.3	0.5
Flat seafloor	0	4	12	33	15	16	20

[a]Areas of scarp, talus, or sediment cover, and sections of the dive where the seafloor was not observed, were omitted from the measurements. Normalized to 100%.

25°N (10–15 cm on the smooth terrains) may have buried any sign of an underlying sheet flow (although this would have required the section of flow covered by the camera to have a much higher pillow density associated with it than observed on sheet and lobate flows at 45°N).

[26] High-resolution studies that ground truth side-scan sonar may in the future open up the possibility of reinterpreting other side-scan data sets from the Mid-Atlantic Ridge. However, the resolution of 30 kHz side-scan sonar is not high enough for there to be any way of distinguishing between a low-relief pillow flow and a lobate or sheet flow.

4.2. Relative Proportions of Morphologies

[27] Relative abundances of each observed lava morphology were estimated and then normalized to sum to 100% (Table 1). Since the dives were not randomly allocated but chosen to cover specific features, this is not a completely unbiased estimate of different lava abundances, but does provide an indication of the percentage of seafloor covered by each flow type. Purely pillow lava flows (pillows + elongate pillows) cover 51% of the surveyed seafloor but are observed either alone or with other lava morphologies on over 77% of the survey area. They are the most common lava morphology and are probably also the most common current eruptive product on the AVR. Sheet flows were observed on only 6–10% of the surveyed seafloor (> 30% in areas of flat seafloor), but are probably underrepresented in the observations as they are easily buried by sediment. Lobate flows are also observed less frequently than pillows, covering 13–43% of the observed seafloor.

[28] Similarities between proportions of different morphologies can be observed between some dives, and this correlates with where the dives were carried out, with marked increases in the proportions of lobate and sheet flows where dives covered areas of flat seafloor. Sheet flows and lobate flows together are observed on > 80% of areas of flat seafloor (Table 2). As we see them only on low-gradient seafloor and they form recognizable flat-looking, uniformly medium-level backscatter seafloor on the 45°N side-scan sonar maps, it is unlikely that the AVR itself has any sheet flows at all on its surface (excluding flat-topped seamounts), while lobate flows occur only on the flatter summits of hummocks.

4.3. Relative Ages

[29] Where pillow and sheet flows can be observed in cross section, the sheet flows appear to have a similar thickness of sediment (usually < 10 cm) lying on their surfaces (e.g., Figure 3o). It is therefore likely that both types of volcanism are occurring in a similar time frame (although not necessarily at the same time). The low exposure of the flat-lying lava flows makes examining the contact relationships between them and the edge of the AVR flank very difficult. Where such contacts are covered by dives, the flat seafloor appears to grade into pillows, appearing first sparsely as single pillows on the surface of the flat lava flow and becoming more common as you get closer to the steep AVR flank. However, there is no evidence of a pillowed flow flowing over the sheet flow, which would cause a sudden change in morphology and gradient, and therefore, it seems likely that the flat-lying flows here on-lap the pillowed flows.

[30] Estimates of regional sedimentation rate in the northern Atlantic vary from ~5 to ~1 cm/kyr [*Emery and Uchupi*, 1984; *Keen and Manchester*, 1970; *Site 410 Shipboard Scientific Party*, 1978; *Stow and Holbrook*, 1984]. These estimates are achieved using different methods (seismic data versus dating of sediment cores), and therefore, the following dates based on sediment thicknesses are given as ranges.

[31] The observed sediment cover on the eastern side of the AVR and in the dive 83 area, which we observe in cross section, suggests that these sheet flows were erupted between 2000 and 10,000 years ago. The other flat-lying lava flow, covered by dive 88, was not observed in cross section so may be older, as mapped by *Searle et al.* [2010]. Since parts of the AVR appear to be as old as 12 kyr [*Searle et al.*, 2010], these young, flat-lying lavas were erupted either during AVR construction or, if the AVR is no longer being built, very shortly afterward. There is no evidence for them being the earliest eruptive products, preceding AVR construction, as suggested elsewhere [e.g., *Parson et al.*, 1993]. These observations are similar to those at 25°N on the Mid-Atlantic Ridge [*Cann and Smith*, 2005] which suggest hummocky terrain and sheet flows being erupted within 5000 years of each other, although unlike at 25°N we get no indication that flows are aging linearly with distance from the ridge crest.

[32] The average differences between SC categories are probably equivalent to between 25 and 50 cm of sediment thickness, which equates to between 5 and 50 ka of sediment deposition. It therefore seems likely that all the lavas were erupted within the last 50 ka and the lavas with the thinnest sediment cover on the southern tip of the AVR may have erupted as late as 2000 ka. These sediment thicknesses and timings are similar to those observed by *Cann and Smith* [2005], despite the different methods used to observe and record sediment coverage.

[33] While using sediment thickness as a dating proxy is an imperfect method, the findings from the sediment dating in this study are consistent with dates presented in *Searle et al*. [2010] from crustal magnetization (< 750 ka for the valley and probably < 10 ka for the AVR) and paleointensity measurements (< 12 ka for the AVR and > 12 ka for the valley floor). *Searle et al*. [2010] also stated that many of the sheet flows on the valley floor are covered with upward of a meter of sediment; however, this is not the case everywhere, and many of the sheet flows simply appear heavily sedimented because they have much lower relief than pillow lavas. Thin sediment cover on sheet flows is observed in cross section in a number of locations and is very unlikely to be the result of a local effect. This is an important observation as it contradicts the conclusion drawn by *Searle et al*. [2010] that all the sheet flows around the AVR are older than the hummocky terrain that builds it. It is however not incompatible with the presented paleointensity data, as none of the samples analyzed in this way were taken from flat areas of seafloor within the inner valley.

5. Conclusions

[34] The main building blocks of AVRs are small hummocks composed almost entirely of pillows. Similar degrees of sediment cover and no obvious overlapping contact relationships suggest that more than one hummock is formed at a time. Pillow lavas are the most common form of volcanism in the 45°N axial valley and are observed almost everywhere, alone or in association with other lava morphologies. Sheet flows are confined to the summits of the large flat-topped seamounts and to areas of flat seafloor surrounding the AVR.

[35] The flat seafloor and the hummocky terrain identified in the side-scan sonar surveys reflect different lava morphologies. Hummocky terrain is mostly composed of pillow and elongate pillow lavas with small amounts of lobate lava flows, while flat seafloor is characterized by higher percentages of sheet and lobate lava flows. This suggests that lavas on and off the AVR were either erupted differently or had different rheology, chemistry, or eruption dynamics.

[36] Both the pillow lava flows on the AVR and the sheet flows around the AVR have similar degrees of sediment cover, suggesting that they were erupted at approximately the same time. There is little variation in the inferred ages of flows on the AVR surface and no obviously contrasting contact relations between different flows, although observations are consistent with the flat seafloor onlapping the AVR flanks. This suggests that most of the lavas observed were erupted in a single period lasting < 50,000 years and that at least some of the flat seafloor is younger than the hummocky AVR.

Acknowledgments

[37] This work was funded by the Natural Environment Research Council (NERC). Yeo acknowledges receipt of an NERC postgraduate studentship. We thank the Shipboard Scientific Party, officers, crew, and technicians of RRS James Cook cruise 24 for their dedication and professionalism in assisting in the data acquisition. The authors also thank Debbie Smith and an anonymous reviewer for their careful reviews, which have greatly improved the manuscript.

References

Aumento, F., Bd. Loncarev, and D. I. Ross (1971), Hudson Geotraverse: Geology of the Mid-Atlantic Ridge at 45 degrees N, *Philosophical Transactions of the Royal Society of London Series A - Mathematical and Physical Sciences*, *268*(1192), 623–651.

Ballard, R. D., and J. G. Moore (1977), Photographic Atlas of the Mid-Atlantic Ridge Rift Valley, Springer, New York, p. 114.

Ballard, R. D., and T. H. Van Andel (1977), Morphology and tectonics of inner rift valley at lat 36degree50'N on Mid-Atlantic Ridge, *Geological Society of America Bulletin*, *88*(4), 507–530.

Bideau, D., R. Hekinian, B. Sichler, E. Gracia, C. Bollinger, M. Constantin, and C. Guivel (1998), Contrasting volcanic-tectonic processes during the past 2 Ma on the Mid-Atlantic Ridge: Submersible mapping, petrological and magnetic results at lat. 34 degrees 52 ' N and 33 degrees 55 ' N, *Marine Geophysical Researches*, *20*(5), 425–458.

Bonatti, E., and C. G. A. Harrison (1988), Eruption styles of basalts in oceanic spreading ridges and seamounts: Effect of magma temperature and viscosity, *J. Geophys. Res.-Sol. Ea.*, *93*(B4), 2967–2980.

Briais, A., H. Sloan, L. M. Parson, and B. J. Murton (2000), Accretionary processes in the axial valley of the Mid-Atlantic Ridge 27 degrees N-30 degrees N from TOBI side-scan sonar images, *Mar. Geophys. Res.*, *21*(1-2), 87–119.

Brown, J., and J. Karson (1988), Variations in axial processes on the Mid-Atlantic Ridge: The median valley of the MARK area, *Mar. Geophys. Res.*, *10*(1), 109–138.

Bryan, W. B., S. E. Humphris, G. Thompson, and J. F. Casey (1994), Comparative volcanology of small axial eruptive centres in the MARK area, *J. Geophys. Res.-Sol. Ea.*, *99* (B2), 2973–2984.

Cann, J. R., and D. K. Smith (2005), Evolution of volcanism and faulting in a segment of the Mid-Atlantic Ridge at 25 degrees N, *Geochem. Geophys. Geosyst.*, *6*, 20.

Chadwick, W. W., and R. W. Embley (1994), Lava flows from a mid-1980s submarine eruption on the Cleft Segment, Juan de Fuca Ridge, *J. Geophys. Res.-Sol. Ea.*, *99*(B3), 4761–4776.

Emery, K. O., and E. Uchupi (1984), The Geology of the Atlantic Ocean, Springer, New York, p. 1050.

Escartin, J., D. K. Smith, J. Cann, H. Schouten, C. H. Langmuir, and S. Escrig (2008), Central role of detachment faults in accretion of slow-spreading oceanic lithosphere, *Nature*, *455* (7214), 790–794.

Flewellen, C., N. Millard, and I. Rouse (1993), TOBI, a vehicle for deep ocean survey, *Electron. Commun. Eng.*, *5* (2), 85–93.

Gente, P., C. Mevel, J. M. Auzende, J. A. Karson, and Y. Fouquet (1989), An example of a recent accretion on the Mid-Atlantic Ridge: The Snake Pit neovolcanic ridge (MARK area, 23-degrees-22'N) *in* Proceedings Symp at the 5th Biennial Meeting of the European Union of Geosciences (Eug-5): The Geology, Geophysics and Metallogeny of the Present-Day Oceans, Strasbourg, France, Mar 20-23, Elsevier Sci., pp. 1-29.

German, C., P. Tyler, and G. Griffiths (2003), The maiden voyage of UK ROV "Isis", *Ocean Challenge*, *12*(3), 16–18.

Goldberg, D., and Y. F. Sun (1997), Attenuation differences in layer 2A in intermediate- and slow-spreading oceanic crust, *Earth Planet. Sci. Lett.*, *150*(3-4), 221–231.

Gràcia, E., L. M. Parson, D. Bideau, and R. Hekinian (1998), Volcano-tectonic variability along segments of the Mid-Atlantic Ridge between Azores platform and Hayes fracture zone: evidence from submersible and high-resolution sidescan sonar data, *Spec. Publ. Geol. Soc. London*, *148*, 1–15.

Gregg, T. K. P., and J. H. Fink (1995), Quantification of submarine lava-flow morphology through analog experiments, *Geology*, *23*(1), 73–76.

Gregg, T. K. P., and J. H. Fink (2000), A laboratory investigation into the effects of slope on lava flow morphology, *J. Volcanol. Geotherm. Res.*, *96*(3–4), 145–159.

Gregg, T. K. P., and D. K. Smith (2003), Volcanic investigations of the Puna Ridge, Hawai'i: Relations of lava flow morphologies and underlying slopes, *J. Volcanol. Geotherm. Res.*, *126*(1-2), 63–77.

Griffiths, R. W., and J. H. Fink (1992), Solidification and morpholoy of submarine lavas: A dependence on extrusion rate, *J. Geophys. Res.-Sol. Ea.*, *97*(B13), 19729–19737.

Karson, J. A., et al. (1987), Along-axis variations in sea-floor spreading in the MARK area, *Nature*, *328*(6132), 681–685.

Keen, M. J., and K. S. Manchester (1970), The Mid-Atlantic Ridge near 45ºN. X. Sediment distribution and thickness from seismic reflection profiling, *Can J. Earth. Sci.*, *7*(3), 735–747.

Keeton, J. A., and R. C. Searle (1996), Analysis of Simrad EM12 multibeam bathymetry and acoustic backscatter data for seafloor mapping, exemplified at the Mid-Atlantic Ridge at 45 degrees N, *Mar. Geophys. Res.*, *18*(6), 663–688.

Kennish, M. J., and R. A. Lutz (1998), Morphology and distribution of lava flows on mid-ocean ridges: A review, *Earth Sci. Rev.*, *43*(3-4), 63–90.

LeBas, T. P. (2005), PRISM - Processing of Remotely-sensed Imagery for Seafloor Mapping - Version 4.0, Southampton National Oceanography Centre.

Macdonald, K. C. (1982), Mid-ocean ridges: Fine scale tectonic, volcanic and hydrothermal processes within the plate boundary zone, *Annu. Rev. Earth Planet. Sci.*, *10*, 155–190.

Mello, S. L. M., J. R. Cann, and C. M. R. Fowler (1999), Anomalous mantle at 45 degrees N Mid-Atlantic Ridge?, *J. Geophys. Res.-Sol. Ea.*, *104*(B12), 29335–29349.

Parson, L. M., et al. (1993), En-echelon axial volcanic ridges at the Reykjanes Ridge: A life-cycle of volcanism and tectonics. *Earth Planet. Sci. Lett.*, *117*(1-2), 73–87.

Searle, R. C., et al. (2010), Structure and development of an axial volcanic ridge: Mid-Atlantic Ridge, 45°N, *Earth Planet. Sci. Lett.*, *299*(1–2), 228–241.

Sempere, J. C., G. M. Purdy, and H. Schouten, (1990), Segmentation of the Mid-Atlantic Ridge between 24-degrees-N and 30-degrees-40'N, *Nature*, *344*(6265), 427–431.

Sinton, J. M., and R. S. Detrick (1992), Midocean ridge magma chambers, *J. Geophys. Res.-Sol. Ea.*, *97*(B1), 197–216.

Site 410 Shipboard Scientific Party (1978), Site 410, *in* Luyendyk, B. P., Cann, J. R., Duffield, W. A., Faller, A. M., Kobayashi, K., Poore, R. Z., Roberts, W. P., Sharman, G., Shor, A. N., Steiner, M., Steinmetz, J. C., Varet, J., Vennum, W., Wood, D. A., and Zolotarev, B. P., eds., Initial Reports of the Deep Sea Drilling Project, Volume 49: National Science Foundation, Washington.

Smallwood, J. R., and R. S. White (1998), Crustal accretion at the Reykjanes Ridge, 61°-62°N, *J. Geophys. Res.*, *103*(B3), 5185–5201.

Smith, D. K., and J. R. Cann (1990), Hundreds of small volcanoes on the median valley floor of the Mid-Atlantic Ridge at 24-30[deg] N, *Nature*, *348*(6297), 152–155.

Smith, D. K., and J. R. Cann (1992), The role of seamount volcanism in crustal construction and the Mid-Atlantic Ridge (24-degrees-30-degrees-N), *J. Geophys. Res.-Sol. Ea.*, *97* (B2), 1645–1658.

Smith, D. K., and J. R. Cann (1993), *Building the crust at the Mid-Atlantic Ridge Nature*, *365*(6448), 707–715.

Smith, D. K., S. E. Humphris, and W. B. Bryan (1995), A comparison of volcanic edifices at the Reykjanes Ridge and the Mid-Atlantic Ridge at 24-degrees-30degrees-N, *J. Geophys. Res.-Sol. Ea.*, *100*(B11), 22485–22498.

Smith, D. K., et al. (1995), Mid-Atlantic Ridge volcanism from deep-towed side-scan sonar images, 25-degrees-29degrees-N, *J. Volcanol. Geotherm. Res.*, *67*(4), 233–262.

Stow, D. A. V., and J. A. Holbrook (1984), North Atlantic contourites: An overview, *Spec. Publ. Geol. Soc. London*, *15*, 245–256.

Wells, G., W. B. Bryan, and T. H. Pearce (1979), Comparative morphology of ancient and modern pillow lavas, *J. Geol.*, *87*(4), 427–440.

White, S. M., R. M. Haymon, D. J. Fornari, M. R. Perfit, and K. C. Macdonald, Correlation between volcanic and tectonic segmentation of fast-spreading ridges: Evidence from volcanic structures and lava flow morphology on the East Pacific Rise at 9°-10° N, *J. Geophys. Res.*, *107*(B8). doi:10.1029/2001JB000571, 2002

Yeo, I., R. C. Searle, K. L. Achenbach, T. P. Le Bas, and B. J. Murton (2012), Eruptive hummocks: Building blocks of the upper ocean crust, *Geology*, *40*(1), 91–94.